EFFECT OF TWIN FUEL INJECTION ON WALL FILM IN MOTORCYCLE ENGINES

Zongzheng MA[1], Haishu MA[2], Liutao HAO[3] and Xinli WANG[4]

Intake port fuel injection (PFI) method is commonly used in gasoline engines, especially those in motorcycles. However, one of the problems of PFI engines is the wall-film, which plays important roles in hydrocarbon emission and fuel economy. Thus, twin fuel injection (TFI) method was applied to PFI motorcycle engines and studied through experiment and simulation to improve wall film evaporation. The influence of TFI parameters, including start of injection timing (SOI) and injection fuel proportion (IFP), on engine performance was investigated for further detail. Results showed that TWI method can improve fuel evaporation compared with single injection. Additional findings show that SOI retardation can decrease wall-film evaporation and lead to engine performance deterioration at part load condition; by contrast, the influence of SOI can be ignored at wide open throttle (WOT) at part load because of increased body temperature. The results also indicated that IFP should be optimized based on engine conditions at part load because its influence on engine performance varies with such conditions; however, the effect of IFP on engine performance at WOT is poor which is also due to its body temperature increase.

Keywords: Motorcycle engine, Gasoline fuel injection, Fuel evaporation, Fuel wall-film, Twin fuel injection, Engine performance

1. Introduction

Compared with direct injection method [1,2], PFI engines remain a popular choice in the automobile industry because of its inherent benefits, such as low fuel quality requirement, manufacturing cost, and particle number emission [3,4]. Particularly in developing areas or countries, the PFI motorcycle engine is preferred due to its convenience and low cost. However, given the increasing attention focused on environment pollution issues, the PFI engines are limited due to its high hydrocarbon (HC) emission and low fuel economy.

One of the most important effects is the wall-film, which performs an important role in the HC emission, fuel economy, and output power of PFI engines [5, 6]. Experimental results indicated that fuel entry into the cylinder in liquid form results in wall-film and leads to high HC emissions because most of the fuel injected into the cylinder in liquid form may not evaporate until ignition

[1] Department of Mechanical Engineering, Henan University of Engineering, China
[2] Department of Mechanical Engineering, Henan University of Engineering, China
[3] Department of Mechanical Engineering, Henan University of Engineering, China
[4] Department of Mechanical Engineering, Henan University of Engineering, China

[7-9]. Meanwhile, an experiment conducted by Kim using visualization methods showed that wall-film is also obtained at the intake port for PFI engines [10]. Posylkin also validated that fuel sprays can directly reach the intake valve and valve seat for PFI engines, and some of the fuel becomes wall-film and is deposited in both areas [11].

Therefore, methods of reducing wall-film are important for PFI gasoline engines. Results from Bianchi, who studied the influence of injection timing on mixture formation by using FIRE software, showed that advanced fuel injection time can effectively reduce wall-film because of extended time for fuel to evaporate and an increasingly homogeneous mixture [12]. The studies conducted by Wang on the basis of a CV20 gasoline engine indicated high body temperature results in minimal wall-film in the cylinder under full load conditions [13]. A similar study involving numerical simulation method conducted by Liu discussed the effect of influencing parameters, including injection pressure, impingement distance from the injector and the impinged wall, injection duration, impingement angle, and wall temperature; results showed that wall-film evaporation increases with the increase in injection pressure, while maximum film thickness decreases with the increase in injection angle [14]. Exhaust-stroke injection, adequate distance from injection to cylinder, and suitable injection timing are beneficial to reduce wall-film [15].

Meanwhile, the intake air flow plays an important role in wall-film formation and evaporation. Nemecek showed that fuel particles can be accelerated by intake air flow and reach the interior of the cylinder, thus preventing the formation of wall-film in the intake port [16]. The same results from Takahashi showed that high intake air velocity can reduce wall-film mass because of high engine speed [17]. The same conclusion was obtained when wall-film development was studied in a mole intake port and expanding corner [18,19]. Additional studies from Schūnemann showed that relative velocity between the intake air and fuel particles is determined by the engine speed and that only fuel particles with small diameter are considerably accelerated by intake air [20].

Thus, another method that can reduce wall film is twin fuel injection (TFI). In TFI proposed by Liu [21,22], the required fuel is injected two times in one cycle; the first injection occurs in the expansion stroke, and the second injection occurs in the intake stroke. This two-time injection also can be referred to as closed valve injection (CVI) and open valve injection (OVI) according to the intake valve state. CVI means that fuel injection occurs in the closed state of the intake valve, whereas OVI means that the action occurs in the intake valve open state. Previous studies showed that the intake air and engine operation conditions exert an important effect on TFI and influence engine output power and emission [23,24].

Owing to their compact intake structure and small cylinder, the motorcycle engines are different from car engines which the TFI applied for. So the influence of TFI parameters, including start of injection timing (SOI) and injected fuel proportion (IFP), on motorcycle engine performance was investigated through experimental and numerical simulation approaches.

2. Experimental research on twin fuel injection strategy

2.1 Experimental apparatus

Fig. 1 shows the schematic of the experimental test bed. The test bed consisted of the motorcycle engine, eddy current dynamometer, dynamometer control system, wide-band oxygen sensor, oxygen sensor measurement system, five-gas analyzer, and engine control unit, which was self-developed based on a micro-chip with serial communication. The type and company of the equipment are shown in Table 1, and the motorcycle engine specifications are listed in Table 2.

An oxygen sensor was mounted in the exhaust pipe, and air-fuel ratio (AFR) was measured using the oxygen sensor measurement system. Engine emission was measured using the five-gas analyzer. As mentioned in the introduction, body temperature exerts an important effect on engine performance and was thus measured using the thermocouple, which was mounted at the spark plug.

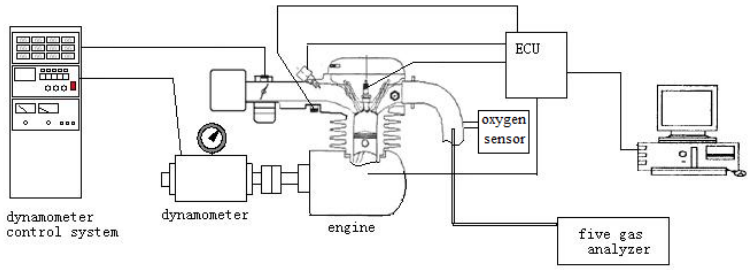

Fig. 1 Schematic diagram of experimental system

Table1

Parameters of the equipments

Equipments	Type	company
Motorcycle engine	K157 FMI	Qingqi Motorcycles Co., Ltd
Eddy current dynamometer	CW22	Hunan Xiangyi Power Testing Instrument Co.,Ltd
Dynamometer Control System	FC2000	Hunan Xiangyi Power Testing Instrument Co.,Ltd
Oxygen sensor	7200LSU	Robert Bosch GmbH
Oxygen sensor measurement	2C0	Tech Edge Co., Ltd.
5 Gas Analyzer	FGA-4100	Foshan Analytical Instrument Co., Ltd.

Table 2

K157 FMI engine parameters

Parameter	Parameter value
Type	Single cylinder, four-stroke
Bore × stroke (mm)	56.5×49.5
Total displacement /L	124
Rated power (kW) / corresponding speed (r / min)	7.0/7500
Compression ratio	9：1
Cooling style	wind cooling

2.2 Experimental procedure

Figure 2 shows the TFI strategy. The first injection refers to fuel injected in the expansion stroke, whereas the second injection denotes the fuel injected in the intake stroke. For TFI, injection timing and fuel proportion affect engine performance, so all effects were investigated using the experiment test bed. For ease of understanding, the top dead center (TDC) of the compression stroke is set as 0º crank angle (CA).The engine was warmed up before testing start. For minimizing its effect, body temperature was maintained constant through the use of a blower. Injection timing was varied via the self-developed engine control unit.

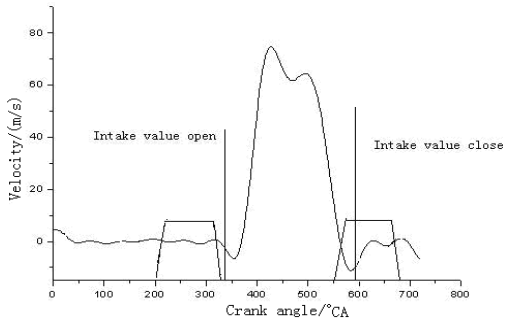

Fig. 2 Twin-fuel-injection strategy

2.3 Effects of SOI of first injection on engine performance

For investigating the effect of SOI of first injection on engine performance, the SOI of second injection was fixed at 320° CA, and the total injection fuel pulse was 8.6 ms with 5.8 mg.

The effects of SOI of first injection on engine power, AFR, and HC emissions when the engine was operated at 4000 r/min and 20% THO state are shown in Figures 3 and 4. Notably, body temperature was maintained at 135 °C to eliminate its influence.

When SOI was postponed, engine output power decreased to 1.92 kW from 1.96 kW, the measured AFR increased to 14.7 from 14.4, and HC emissions increased to 843×10^{-6} from 764×10^{-6}. Thus, delayed injection timing leads to engine performance deterioration.

Meanwhile, the effects of injection timing on engine performance changed when the engine was operated in wide open throttle (WOT) state and the engine speed was kept constant (Figs. 5 and 6). At this time, body temperature was maintained at 155 °C, and the total injection fuel pulse was 11 ms with 7.0 mg.

Therefore, engine output power, measured AFR, and HC emissions were not significantly changed when the first SOI varied from 10° CA to 150 °CA. This finding suggests that injection timing does not affect engine performance at WOT state.

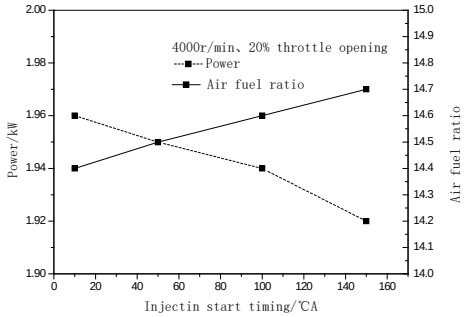

Fig.3 Effects of SOI of first injection on engine power and AFR at 4000r/min and 20%THO

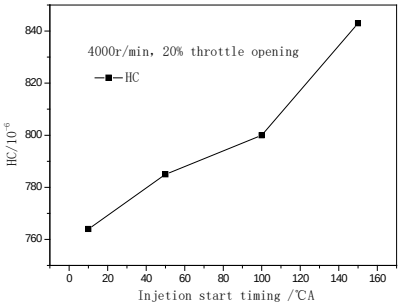

Fig. 4 Effects of SOI of first injection on HC emissions at 4000r/min and 20% THO

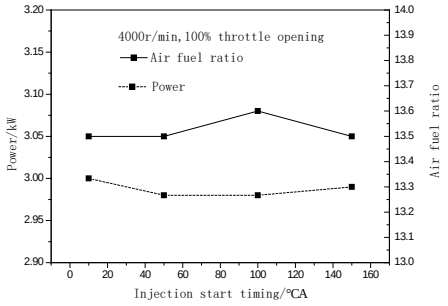

Fig. 5 Effects of SOI of first injection on power and AFR at 4000r/min and WOT

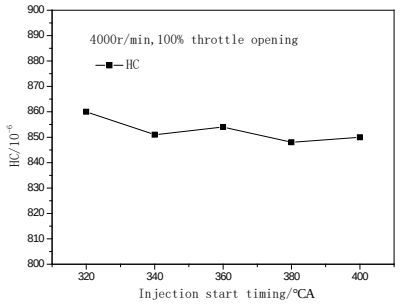

Fig. 6 Effects of SOI of first injection on HC emission at 4000r/min and WOT

2.4 Effects of SOI of second injection on engine performance

For analyzing the influence of SOI of second injection on engine performance, the SOI of first injection was fixed at 40 °CA. The experiment was conducted under the same conditions mentioned above.

When the SOI was varied from 320° CA to 400° CA, engine output power decreased by 0.2 kW, measured AFR increased to 15.3, and HC emissions also increased to 890×10^{-6} from 860×10^{-6} at 20% THO (Figs. 7 and 8).

The effects of SOI of second injection evidently show the same trend as the first injection timing at WOT (Figures 9 and 10), with the values between the two conditions being the only difference.

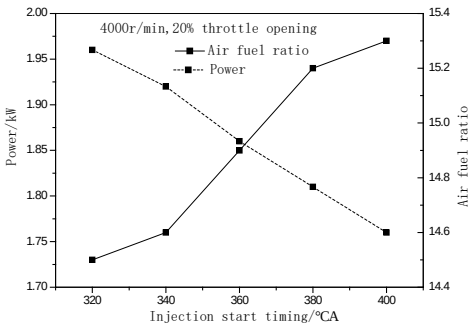

Fig. 7 Effects of SOI of second injection on power and AFR at 4000r/min and 20% THO

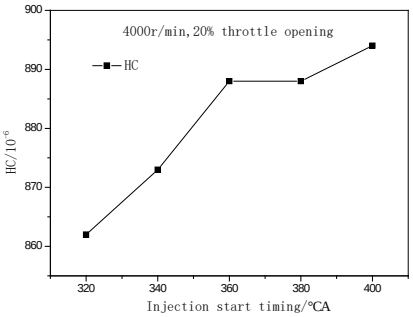

Fig. 8 Effects of SOI of second injection on HC emission at 4000r/min and 20% THO

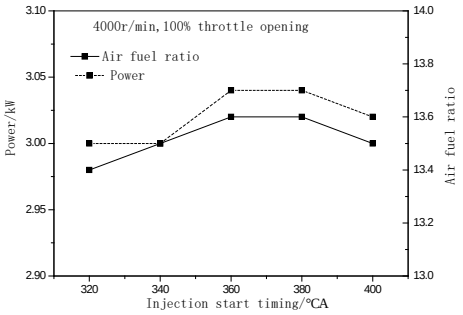

Fig. 9 Effects of SOI of second injection on power and AFR at 4000r/min and WOT

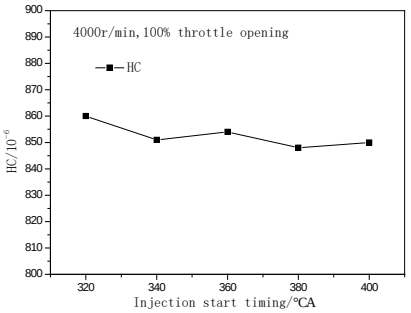

Fig. 10 Effects of SOI of second injection on HC emission at 4000r/min and WOT

2.5 Effect of fuel proportion on engine performance

For investigating the effects of fuel proportion on engine performance, the SOI of first injection was fixed at 40 ºCA, and the SOI of second injection was fixed at 320º CA. Injection pulse width was simultaneously adjusted to maintain the same fuel quality according to nozzle injection calibration. Table 3 shows the effect of fuel proportion on engine performance when the engine is operated at 4000 r/min and 20% THO. Engine output power was 1.95 kW when the first and second fuel injection pulse widths were set at 6 and 2.6 ms, respectively. However, the engine output power was only 1.91 kW when the injection pulses width was exchanged.

The same output power trend was observed when the pulse widths of the first and second fuel injection were set at 4.3 ms. Meanwhile, the values of torque and measured AFR also changed, indicating that first fuel injection pulse width is directly proportional to engine performance. Similarly, the same conclusion can be obtained at the WOT state, as shown in Table 4.

Table 3

Effects of fuel proportion on power at 4000r/min and 20% THO

First injection pulse width/ms	second injection pulse width /ms	Power/kW	Torque/N·m	AFR
4.3	4.3	1.91	14.8	14.6
5	3.6	1.94	14.7	14.5
3.6	5	1.93	14.6	14.7
6	2.6	1.95	14.7	14.4
2.6	6	1.91	14.5	14.8

Table 4

Effects of fuel proportion on power at 4000r/min and WOT

First injection pulse width /ms	second injection pulse width /ms	Power/kW	Torque/N·m	AFR
5.5	5.5	3.49	21.2	13.9
6	5	3.48	21.3	13.9
5	6	3.47	21.1	14.1
7	4	3.49	21.1	13.9
4	7	3.42	20.9	14.2
3	8	3.4	20.6	14.3
8	3	3.5	21.1	13.9

From experiment above, we can conclude that the relationship among injection timing, fuel proportion, and engine performance varies with engine operation condition; however, the relationship cannot be explained by the experiment. Thus, numerical analysis was conducted based on the experiment. The relationship among injection timing, fuel proportion, and engine performance under different operation conditions was analyzed.

3. Numerical analysis

3.1 Model Development and Validation

The engine used for studying is a four-stroke wind cooling motorcycle engine, and the motorcycle engine specifications are listed in Table 2. According to the actual size of the engine, one 3D model of the intake port and combustion charmer was established based on Solidworks platform and then meshed with FAME technology based on FIRE software.

For reducing grid number and computation time, three different meshes were used to simulate the processes of fuel injection and air–fuel mixing. The meshes can be seen in Figure 11. When the intake valve is closed and fuel injection occurs in the intake port, the fuel injection and air–fuel mixing can be simulated by the intake port mesh (Fig. 11.a). When the intake valve is opening and the fuel–air mixture is entering the combustion chamber, the process can be simulated by the intake and combustion chamber mesh (Fig. 11.c). When the intake valve is closed and the fuel–air mixing process is ongoing in the combustion chamber, the process can be simulated only by the combustion chamber mesh (Fig. 11.b).

(a) Intake port mesh

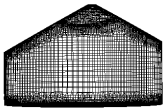

(b)Combustion chamber mesh

(c) Intake and combustion chamber mesh

Fig. 11 Mesh for the simulation

For PFI gasoline engine simulation, the most important models were the spray and wall-film models. So the fuel spray process was simulated by Dispersion Droplet model and the wall impingement process was simulated by Mundo Sommerfeld model. Then the models were validated using schlieren method based on constant volume. And its schematic diagram is shown in figure 12 and the specifications of the experiment are listed in table 5[23].

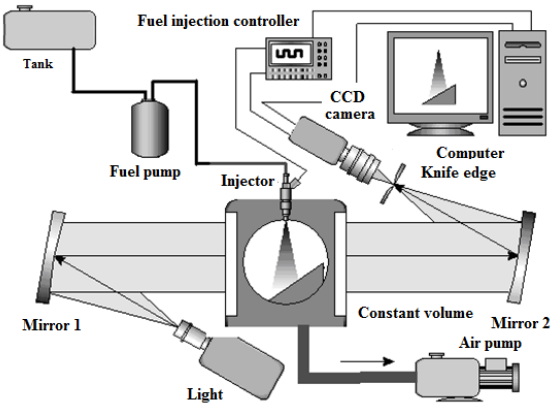

Fig. 12 Schematic diagram of the schlieren method

The schlieren system consists of a xenon lamp as the light source, two mirrors, a knife edge, a high speed camera and a signal acquiring system. As the experiment start, the point-light became Parallel-light through the mirror 1 for lighting. When the fuel is introduced into the observation area, it will change the gradient of the area. Therefore, this difference in gradient will be received by the high speed camera and then send to the computer by the signal acquiring system.

Table 5

Specification of the experiment

Content	Parameters	Content	Parameters
Schlieren light source	150W Xenon lamp	Injection press	0.3MPa
Camera	Shutter:1/50000s;Resolution:656x490	Ambient condition	0.1MPa
Mirror	D=150 mm, f=1500 mm	Ambient temperature	25℃
Screen (Avenir TV SL 08551）	f:8.5-51mm, F1.2	Wall temperature	25℃
Nozzle	Sigle,Diameter:0.2mm	Injection duration	3ms

Figure 13 is the comparison of fuel spray and wall impingement process with schlieren method and numerical method at the same conditions. It shows that the spray and wall impingement process predicted by the model has a good agreement with the experimental results at 3ms, 7ms after the start of fuel injection. Therefore, the model can be used to determine the effect of engine control parameters on the oil film attached to the wall.

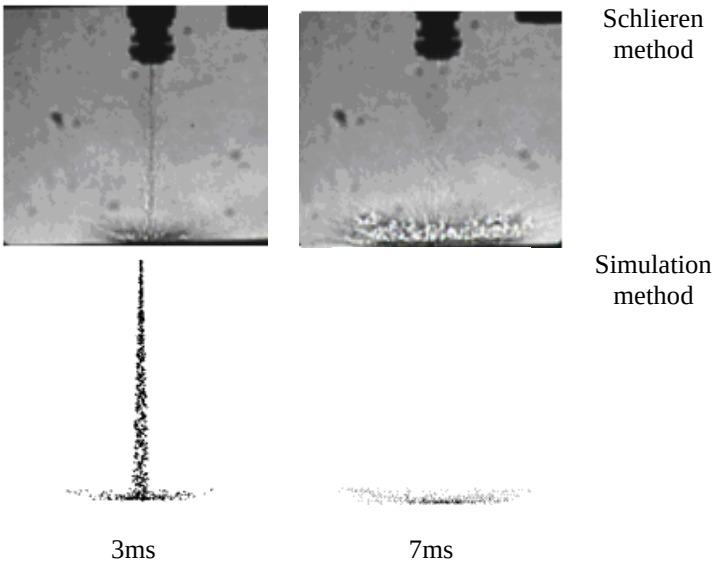

Fig. 13 Comparison of fuel spray and wall impingement process

3.2 Initial and boundary conditions set

Initial and boundary conditions, such as intake port temperature, intake air temperature, valve temperature, combustion chamber temperature, and residual gas temperature, were set based on the measured data from the experiment engine, and their values are shown in Table 6. Notably, we selected only two operation conditions, 20% THO and WOT, which represent the different typical operation conditions at 4000 r/min. For ease of comparison, fuel injection pulse width remained at 2.5 ms with a mass of 2.63 mg for different throttle openings, and the difference under actual operating conditions were not considered.

Table 6

Initial and boundary condition sets

Content	Parameters	Value at 20% THO	Value at WOT
Boundary condition	Intake port temperature	80° C	100° C
	Intake valve temperature	100° C	120° C
	Combustion chamber temperature	137° C	158° C
Initial condition	Intake air temperature	20° C	20° C
	Intake air pressure	90kPa	100kPa
	Residual gas temperature	750° C	800° C
	Residual gas pressure	95kPa	100kPa

3.3 Results and discussion

On the basis of previous research, fuel evaporation can be divided into space evaporation and wall-film evaporation, which represent the fuel evaporated during injection and evaporated from the wall-film.

3.3.1 Effects of SOI of first injection on wall-film

For investigating the influence of SOI of first injection on engine performance, the SOIs were set at 20º, 40º, and 60° CA.

(1) 20% THO state

Fig. 14 illustrates the wall-film evaporation mass comparison of different SOIs at 20% THO. At 700º CA, the wall-film evaporation mass was 1.44 mg when SOI was set at 20º CA, whereas wall-film evaporation mass was only 1.35 mg when SOI was postponed to 60º CA, and the mass difference was 0.09 mg. Fuel injection time is 2.5 ms, corresponding to about 240° CA at 4000 r/min speed. Therefore, the intake valve is closed when the injection process is completed even with SOI is set at 60º CA. No intake air flow occurs, and wall-film evaporation is mainly based on absorbing heat through the inlet wall. Logically, SOI retardation decreases wall-film evaporation because it reduces wall-film evaporation time.

However, wall-film evaporation is not completed in the intake valve closed state. Figure 14 shows that wall-film evaporation mass still increases when the intake valve is open (about at 360° CA); wall-film evaporation mass rate also increases, as observed from the wall-film mass curve slope. Therefore, intake air flow is an important factor for promoting wall-film evaporation because of the interaction between the intake air and wall-film.

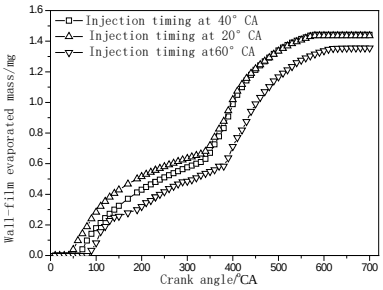

Fig. 14 Comparison of wall film evaporated mass for different SOIs at 20%THO

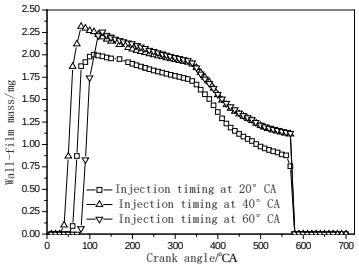

Fig. 15 Comparison of wall film mass for different SOIs at 20%THO

Figure 15 shows that liquid mass increases when SOI is delayed. SOI delay leads to additional liquid fuel in the intake port. Given all SOI states, wall-film was still observed in the intake port at 570° CA when the intake valve was closed, suggesting the presence of some liquid fuel in the intake port that was possibly introduced into the combustion chamber through the intake valve gap. This part of liquid fuel may not evaporate during the compression stroke and thus exhaust the engine, resulting in increased HC emissions. Then, this portion is added fuel that cannot be combusted and consequently leads to engine performance deterioration.

In addition, Fig. 15 shows that the maximum wall-film mass value is about 2.4 mg, which is nearly 91% of the injected fuel; therefore, space evaporation can be disregarded.

(2) WOT state

As seen from the initial and boundary conditions sets, body temperature does not rise at WOT state when engine speed remains unchanged. For comparing the influence of SOI, the injected fuel mass is consistent with 20% THO.

Figure 16 shows the wall-film evaporation mass comparison of different SOIs at WOT. In the figure, the wall-film evaporation mass is 2.35 mg at 700° CA immediately before ignition when SOI is 20° CA; by comparison, wall-film evaporation mass is 2.32 mg when SOI is postponed to 60° CA. The percentages of evaporated wall-film mass are 90% and 87% of injected fuel, meaning that the effects of SOI can be negligible in the WOT state because high body temperature can reduce the influence of injection timing.

The effects of SOI on engine performance can also be seen from figure 17 which shows the wall-film mass comparison for different SOIs at WOT. Only 0.2 mg of wall-film, which accounts for about 7% of the injected fuel, remains in the intake port when the intake valve is closed; this value is approximately 48% at 20% THO.

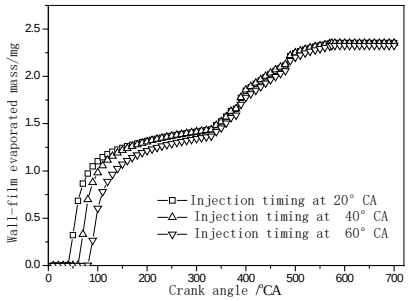

Fig. 16 Comparison of wall film evaporated for different SOIs at WOT

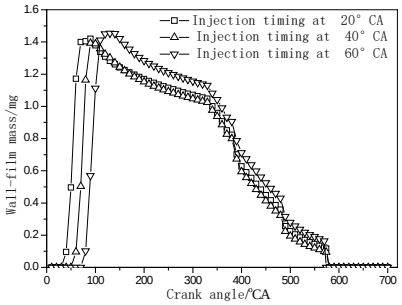

Fig. 17 Comparison of wall film for different SOIs at WOT

3.3.2 Effects of SOI of second injection on wall-film

When the intake valve is opened, intake air is introduced into the combustion chamber, and fuel and intake air interact if the fuel is injected during the intake stroke. Then, the fuel spray is deflected, and spray location changes as shown in Figure 18, which illustrates spray comparison in different injection modes.

Fuel particles in the flow direction show a sub-velocity when intake air is introduced, and fuel can be distributed in a wide area for the OVI mode. In this mode, fuel evaporation during injection cannot be negligible because of the interaction between the fuel and intake air. Therefore, the second injection can be considered as the OVI mode. Wall-film evaporation and fuel evaporation were

considered when the effects of second injection timing on wall-film was studied, and the second SOIs were set at 320°, 360°, and 400° CA.

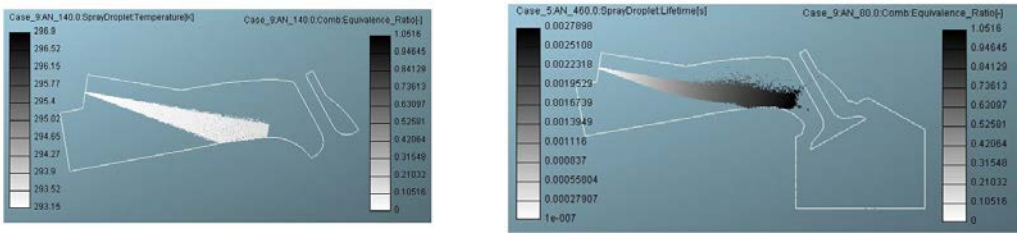

（a）CVI （b）OVI

Fig. 18 Comparison of the fuel spray at different injection mode

(1) 20% THO state

Figure 19 depicts the space evaporation comparison of different SOIs at 20% THO. Space evaporation mass is 0.79 mg at 700° CA before ignition when SOI is 320° CA, whereas the space evaporation mass is only about 0.25 mg for other SOIs.

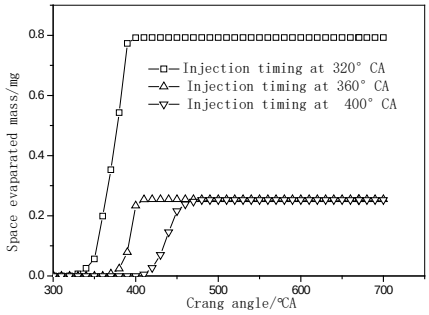

Fig. 19 Comparison of space evaporated mass for different SOIs at 20% THO

This finding can be explained by Figure 20, which shows spray and temperature for different SOIs at 20% THO. Some of the fuel reflects back to the intake port and meets intake air again at a sufficiently high intake air velocity at the beginning of the intake valve opening, thus resulting in increased space evaporation mass when SOI is 320° CA. Meanwhile, most of the injected fuel reaches the combustion chamber directly and becomes wall-film because of the relative low velocity between air and fuel for the other two SOIs. Thus, the space evaporation difference appears.

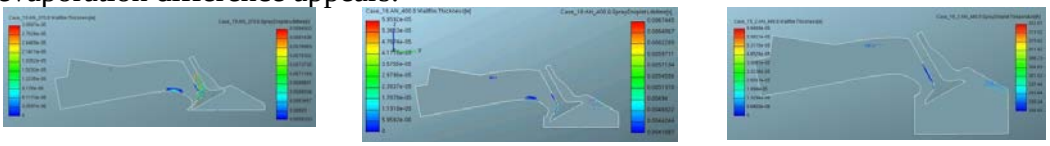

（a）SOI is 320°CA （b）SOI is 360°CA （c）SOI is 400°CA

Fig. 20 Spray and temperature for different SOIs at 20%THO

Fig. 21 is the wall-film evaporation mass comparison of different SOIs at 20% THO. The wall-film evaporation mass is 1.63 mg at 700° CA immediately before ignition when SOI is 360° CA, whereas wall-film evaporation mass is only 0.91 mg when SOI is 400° CA. According to foregoing analysis, intake airflow can increase fuel evaporation rate. Intake air velocity is high when SOI is 320° or 360° CA, thereby potentially increasing wall-film evaporation. By contrast, intake air velocity is relatively low when SOI is set at 400° CA, leading to small wall-film evaporation mass.

Notably, the injected fuel is located in two different regions, namely, the back of intake valve and the combustion chamber wall (Figure 20). This phenomenon can also be found in Fig. 22, which shows the comparison of wall-film for different SOIs at 20% THO.

Wall-film mass considerably decreases at 580° CA when the simulation mesh is changed to combustion chamber mesh (Figure 11). This finding means that some wall-film mass remains in the intake port. Meanwhile, 0.51 mg of wall-film is retained in the combustion chamber especially when SOI is set at 400° CA. This portion of wall-film mass may not evaporate due to short evaporation time.

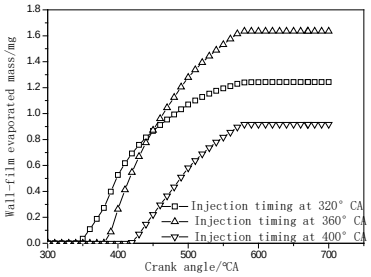

Fig. 21 Comparison of wall film evaporated mass for different SOIs at 20% THO

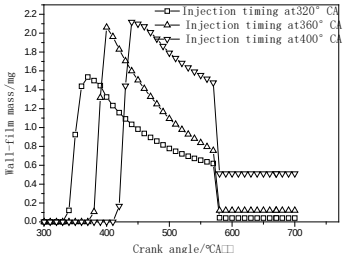

Fig. 22 Comparison of wall film for different SOIs at 20% THO

Then, the total fuel evaporated for different SOIs is shown in Figure 23. When SOI is 320° CA, the sum of the evaporated fuel is the maximum value, whereas the sum of the evaporated fuel when SOI is 400° CA is the minimum value. Then, engine performance and HC emission may deteriorate because of decreased fuel evaporation.

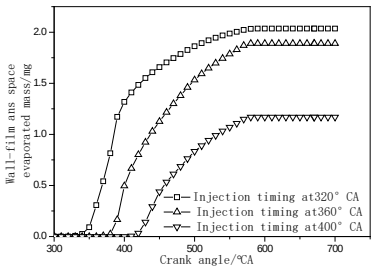

Fig. 23 Comparison of sum evaporated fuel for different SOIs at 20%THO

(2) WOT state

Fig. 24 shows the space evaporation comparison of different SOIs at WOT. Space evaporation mass values are 0.85 mg at 700° CA before ignition and at a SOI of 320 ºCA and 0.40 mg for the other two SOIs. Fig. 25 is the wall-film evaporation comparison of different SOIs under the same operation conditions. The wall-film evaporation mass is 1.70 mg at 700° CA and SOI of 320º CA, whereas the other two SOIs present wall-film evaporation mass values of 2.10 and 1.91 mg.

The sum of space evaporation and wall-film evaporation is shown in Figure 26. The value for the 320° CA SOI is the maximum (2.60 mg), whereas the minimum of 2.3 mg is obtained at 400 ºCA SOI. In comparing the injected fuel, 87% of injected fuel evaporated for all SOIs at WOT. Therefore, injection timing exert virtually no effect on engine performance at WOT when the engine operated at 4000r/min (Figs. 9 and 10).

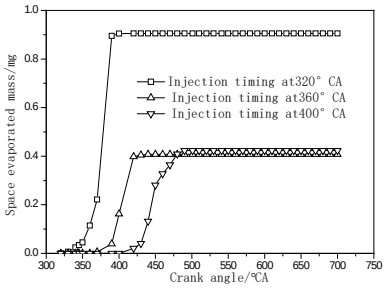

Fig. 24 Comparison of space evaporated mass for different SOIs at 20% THO

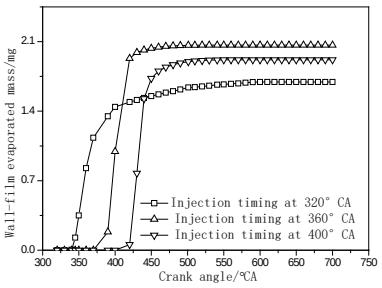

Fig. 25 Comparison of wall-film evaporated mass for different SOIs at 20% THO

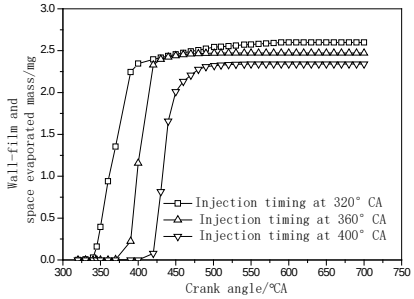

Fig. 26 Comparison of wall film and space evaporated mass for different SOIs at 20%THO

3.3.3 Effects of fuel proportion on fuel evaporation

Following the foregoing analysis, we studied the effect of fuel proportion based on different operation conditions. The SOIs of first and second injection are fixed at 40° and 320° CA, respectively. In the analysis, single injection is also calculated when all of the fuel is injected in CVO mode.

(1) 20% THO

Fig. 27 shows the comparison of space evaporation for different injection ratios at 20% THO. At the fuel injection ratio of 1:3 (first injection is the first part), space

fuel evaporation was 0.10 mg; this value changed to 0.30 mg when the fuel injection ratio was 1:1. For the single injection mode, the value was only 0.06 mg. A large amount of fuel injected in the first injection leads to small space fuel evaporation. This trend is attributed to most of the fuel injected during first injection reaching the intake port wall and forming wall-film because of static air in the intake port.

Figure 28 shows the comparison of wall-film evaporation for different injection proportions. The figure shows that the maximum value of wall-film evaporation is 1.50 mg when the injection ratio is 1:1, whereas the minimum value is 1.35 mg when injection ratio is 1:3; this value is smaller than that in single injection mode. Before the intake valve is opened, wall-film evaporation depends mainly on heat absorption from the intake port wall, and wall-film evaporation rate is almost same. When the intake valve is opened, the effect of intake air becomes the main factor for wall-film evaporation. The interaction of intake air and wall-film is determined by relative velocity and wall-film mass. With low relative velocity and small wall-film mass, wall-film evaporation mass is correspondingly small.

At the injection ratio of 1:3, additional fuel is injected during the intake stroke, and the wall-film evaporation value is small because of slow velocity. Meanwhile, the injection ratio of 3:1 yields a small wall-film amount, resulting in low wall-film evaporation. The maximum value of wall-film evaporation can be reached at the fuel injection ratio of 1: 1.

Figure 29 shows the sum of space evaporation and wall-film evaporation. The sum is 1.85 mg, which is nearly 70% of injected fuel, at the injection ratio of 1:1; however, this value is 1.47 mg, which is less than 50% of injected fuel, when the injection ratio is 1:3. The value is 1.68 and 1.52 mg for the injection ratio of 3:1 and single injection, respectively. Only the value obtained at a ratio of 1:3 is less than that of the single injection mode.

These results suggest that TFI can improve fuel evaporation compared with single injection, but the injection ratio should be optimized.

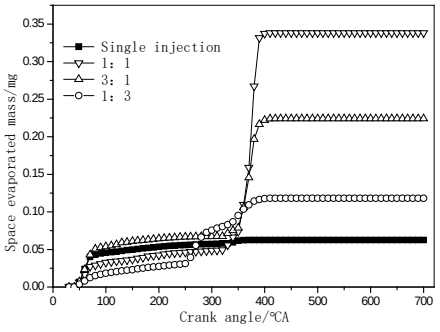

Fig. 27 Space evaporation for different fuel proportion at 20%THO

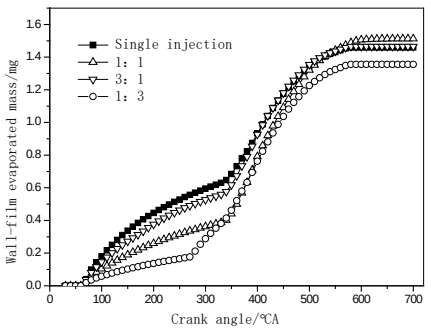

Fig. 28 Wall film evaporation for different injection ratio at 20%THO

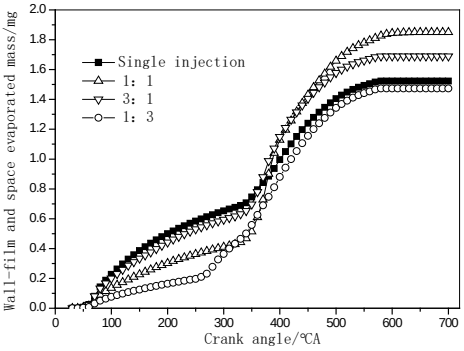

Fig. 29 Comparison of wall film and space evaporated mass for different proportion at 20%THO

(2) WOT state

For the W O T state, only the sum of space evaporation and wall-film evaporation is compared (Figure 30). The injected fuel is 12 mg under this condition.

The difference between the maximum and minimum values is 1 mg, which is approximately 8% of the total injected fuel. The minimum value appears at the injection ratio of 1:3, meaning that the second injection should cooperate with intake air and that additional fuel injected in the second time yields poor results.

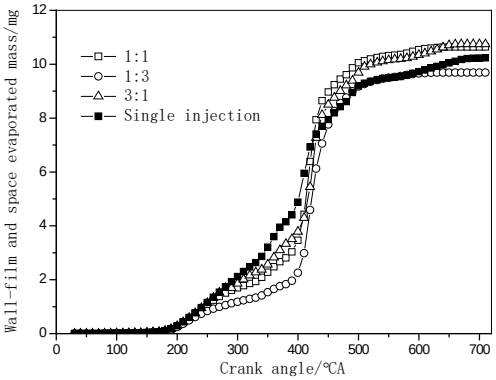

Fig. 30 Comparison of wall film and space evaporated mass for different injection ratio at WOT

4 Conclusion

In this paper, TFI was applied to a motorcycle engine, and the effects of influence parameters, such as SOI, IFP, and operation condition, on engine performance were investigated. The following conclusions are derived from those investigations.

1) The SOI of first injection delay at TFI model can lead to engine performance deterioration when the engine operates at part load due to less wall-film evaporation. So the first SOI should be set at compression stroke in order to improve wall-film evaporation and reach good engine performance.

2) There are no effects on engine performance of SOI under WOT condition when the engine operated at part load because of the high wall-film evaporation reached due to the increased body temperature.
3) Compared with single injection, the sum of space evaporation and wall-film evaporation for TFI is bigger when the injection ratio is 1:1, 3:1 at 20% THO, but the value is smaller when the injection ratio is 1:3. So in order to improve the fuel evaporation the second injection part should be small than the first injection part.
4) When the engine operates at WOT condition, the difference of fuel evaporation between the maximum and minimum values is approximately 8% of the total injected fuel when the injection ratio varies. So the TFI method has poor effect on engine performance at WOT condition and part load condition.

Acknowledgement

This work was supported by Young key teachers Supporting Project of Henan Province (2014GGJS-120). The authors would like to express appreciation of financial support by the Henan Province Engineering research Center for Simulation Test of Coating Production Line.

REFERENCES

[1] *Kim T, Song J, Park S.* “Effects of turbulence enhancement on combustion process using a double injection strategy in direct-injection spark-ignition (DISI) gasoline engines”, International Journal of Heat & Fluid Flow, 2015, 56(3):124-136.
[2] *Keskinen K, Kaario O, Nuutinen M, et al.* “Mixture formation in a direct injection gas engine: Numerical study on nozzle type, injection pressure and injection timing effects. Energy”, 2016, 94:542-556.
[3] *Iorio S D, Sementa P, Vaglieco B M.* “Experimental Characterization of an Ethanol di - Gasoline PFI and Gasoline di - Gasoline PFI Dual Fuel Small Displacement SI Engine”, Sae Technical Papers, 2015, 2015(12):1835-1848.
[4] *Cocchi A, Andreini P, Cassitto L, et al.* “Evaluation of the Effects of a Twin Spark Ignition System on Combustion Stability of a High Performance PFI Engine”, Energy Procedia, 2015, 81:897-906.
[5] *Claret J, Lauer T, Bobicic N, Posselt A et al..* "Impact of the Injection and Gas Exchange on the Particle Emission of a Spark Ignited Engine with Port Fuel Injection," SAE Technical Paper 2017-01-0652, 2017.
[6] *Brehm, C., et al.* “Air and Fuel Characteristics in the Intake Port of a SI Engine. Peterson's graduate and professional programs, an overview”, Peterson's, 1999:269-77.
[7] *Stanglmaier, R H, Hall M J, and Matthews R D.* "In-Cylinder Fuel Transport During the First Cranking Cycles in a Port Injected 4-Valve Engine." International Congress & Exposition 1997.
[8] *Claret J, Lauer T, Bobicic N, Posselt A et al.,* "Impact of the Injection and Gas Exchange on the Particle Emission of a Spark Ignited Engine with Port Fuel Injection," SAE Technical Paper 2017-01-0652, 2017.
[9] *Kalantari, D., and C. Tropea.* "Liquid spray impact onto flat and rigidwalls: Formation and spreading of accumulatedwall film." Fluid Dynamics & Materials Processing 10.1(2014):37-

61.
[10] *Kim H, Yoon S, and Lai M C, et al.* "Correlating Port Fuel injection to Wetted Fuel Footprints on Combustion Chamber Walls and UBHC in Engine Start Processes." SAE Powertrain & Fluid Systems Conference & Exhibition 2003.
[11] *Posylkin, M., Taylor, A., Vannobel, F., and Whitelaw, J.*, "Fuel Droplets Inside a Firing Spark-Ignition Engine," SAE Technical Paper 941989, 1994.
[12] *Bianchi G, Brusiani F, Postrioti L, Grimaldi C, et al.*. "CFD Analysis of Injection Timing Influence on Mixture Preparation in a PFI Motorcycle Engine," SAE Technical Paper 2006-32-0022, 2006,
[13] *Wang X Y, Chen G H.* "Three-dimensional transient simulation of air-fuel mixture process in PFI gasoline engine", Journal of HuaZhong University of Science and Technology (Natural Science edition), 2007, 35(6):92-95.
[14] *Liu H, et al*. "Three-dimensional numerical investigation on wall film formation and evaporation in port fuel injection engines." Numerical Heat Transfer Applications 69.12(2016):1-18.
[15] *Yu J, Abe M, Sukegawa Y. A* "Numerical Method to Simulate Intake-Port Fuel Distribution in PFI Engine and Its Application", WCX™ 17: SAE World Congress Experience. 2017.
[16] *Nemecek, L. M., Wagner, R. M., et al*. "Fuel and Air Studies for Spark Ignition Engine Cold Start Applications", Proceedings of ILASS-America, pp.191-195.
[17] *Takahashi Y, Nakase Y, and Ichinose H*. "Analysis of Fuel Liquid Film Thickness on the Intake Port of a Port Fuel Injection Engine." SAE 2006 World Congress & Exhibition 2006:177-202.
[18] *Zhang Y, Jia M, Duan H, Wang, P et al*., "Experimental and Numerical Study of the Liquid Film Separation and Atomization at Expanding Corners," SAE Technical Paper 2017-01-0856, 2017.
[19] *Ge H, Zhao P*. "Fuel wall film effects on premixed flame propagation, quenching and emission", Us National Combustion Meeting. 2017
[20] *Schūnemann E, Münch K U, and Leipertz A*. "Interaction of Airflow and Injected Fuel Spray Inside the Intake Port of a Six Cylinder Four Valve SI Engine." International Fuels & Lubricants Meeting & Exposition 1997.
[21] *Pei P C, Liu S L, Fan Y J."* A Study on the In-Port Twin Fuel Injection Mode in a 5-Valve S. I. Engine", Transaction of Csice, 2000, 18(1):53-56.
[22] *Liu D X, Feng H Q, Liu S L, et al*. "Experimental Study on the Effects of Twin Fuel Injection Process on Performance of Lean Burn Gasoline Engine", Transactions of Csice, 2003, 21(5):333-336.
[23] *Ma Z, Chen Y, Ji S, et al*. Influences of Intake Flow on Spray and Wall-film for Port Fuel Injection Gasoline Engine. Transactions of the Chinese Society for Agricultural Machinery,2012,43(3): 10-15+27.
[24] *Ma Z, Xu P, Wang X, et al,*. Analysis of Fuel Evaporation for PFI Gasoline Engine at High Engine Body Temperature. UPB Scientific Bulletin, Series D: Mechanical Engineering,2017,79(1):107-118.